Low Grashof Number Convective Heat Transfer across a Spherical Cavity

G. D. McBain and D. W. Stephens

School of Engineering, James Cook University, Townsville QLD 4811

Abstract

The increase in the heat transfer rate across a spherical fluid-filled cavity embedded in a highly conducting solid with a horizontal temperature gradient is investigated analytically and numerically. Analytically, the low Grashof number asymptotic expansion is extended to second-order for the temperature field. This provides the lowest order correction to the overall Nusselt number. This prediction and the associated flow and temperature fields are compared with specially obtained numerical solutions of the full nonlinear equations. Agreement is excellent for Rayleigh numbers less than a few thousand.

1. Introduction

Natural convection in horizontally heated cavities is a much studied subject [1]. Although all real cavities are three-dimensional, the early work [2, e.g.] tended to treat the problem as two-dimensional. Two directions have an obvious physical significance: the directions of gravity and the applied heating ($-y$ and $-x$, in figure 1 a). If the extent of the cavity in the third (z) direction is large, it was argued that the finitude of the span would have little effect on the overall flow or heat transfer. This assumption remained unchallenged until the numerical solutions of Mallinson and de Vahl Davis [3, 4] revealed that the walls bounding a rectangular cavity in the spanwise direction actually profoundly affect the flow throughout the cavity, generating an appreciable axial motion along the primary convective roll. These results, which were featured in the opening keynote paper of the previous conference in this series [5], have been confirmed by flow visualization [6, 7].

The physical mechanisms responsible for the secondary three-dimensional flow have been further illuminated by consideration of the analogous, but analytically more tractable, problem of convection in a horizontally heated *spherical* cavity [8, 9]. Convection in spheres had been analysed by Lewis [10] and Ostroumov [11], though they both wrongly assumed that the flow was confined to planes normal to the z-axis.

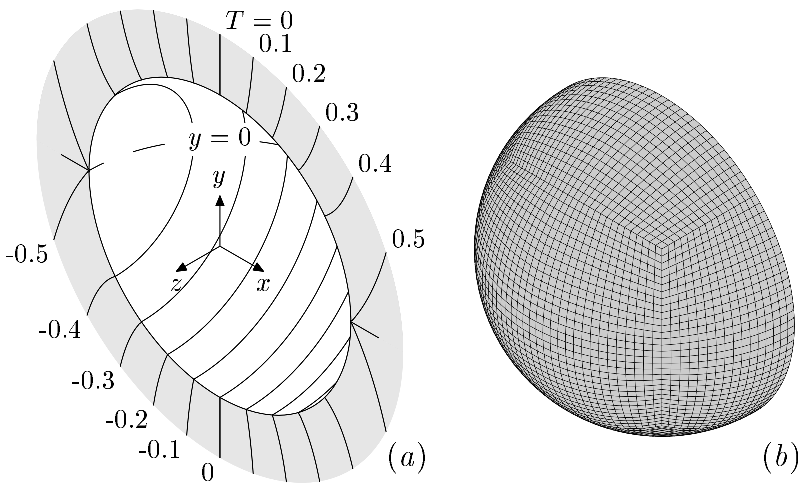

Figure 1: The geometry, sliced in the plane of symmetry $z = 0$, showing (a) thermal boundary conditions and (b) the discretization into hexahedra. In (a), the surface of the cavity is white and concave while the section through the exterior is shaded.

Asymptotic results up to $O(Gr^2)$ have been presented [9], but to this order the overall heat transfer rate is identical to that which would obtain under pure conduction. The present paper extends the asymptotic expansion for temperature to $O(Gr^3)$ and so allows calculation of the first nonzero correction to the heat transfer rate. This prediction, along with the approximations for the flow and temperature fields, is then here compared with newly obtained numerical solutions of the full nonlinear governing equations.

2. General Model

Natural convection is taken to be governed by the Boussinesq equations of motion and heat. These contain two parameters: the Grashof number, $Gr = g\beta\Delta T D^3/\nu^2$; and the Prandtl number, $Pr = \nu/\kappa$. Here, g is the gravitational acceleration, β the thermal coefficient of volumetric expansion, ΔT the imposed temperature difference, D the diameter of the sphere, and ν and κ the fluid's kinematic viscosity and thermometric conductivity. Taking D, ρD^3, $D^2/\nu Gr$ and ΔT as the scales of length, mass, time and temperature, the nondimensional steady-state equations are:

$$
\begin{aligned}
\boldsymbol{\nabla} \cdot \mathbf{u} &= 0; && (1)\\
Gr\, \mathbf{u} \cdot \boldsymbol{\nabla} \mathbf{u} &= -\boldsymbol{\nabla} p + T\hat{\boldsymbol{\jmath}} + \boldsymbol{\nabla}^2 \mathbf{u}; && (2)\\
Gr Pr\, \mathbf{u} \cdot T &= \nabla^2 T, && (3)
\end{aligned}
$$

where $\hat{\boldsymbol{\jmath}}$ is the unit vertical vector, $\mathbf{u}$ is the velocity, T is the temperature and p is the excess of the pressure over its hydrostatic value.

In addition to the Cartesian coordinate system depicted in figure 1 (a), spherical–polar systems with respect to both the z, (r, θ, ϕ), and y, (r, η, υ), axes will be required. These are defined by: $x = r\sin\theta\cos\phi = r\sin\eta\sin\upsilon$; $y = r\sin\theta\sin\phi = r\cos\eta$; and $z = r\cos\theta = r\sin\eta\cos\upsilon$.

The walls, $r = \frac{1}{2}$, are impermeable and nonslip, so that $\mathbf{u} = \mathbf{0}$ there. As thermal boundary condition, we use

$$T = x, \qquad (r = \tfrac{1}{2}). \tag{4}$$

As discussed elsewhere [8, 9], this is a good approximation in so far as the surrounding solid is a much better thermal conductor than the fluid. The temperature field $T = x(16 + r^{-3})/24$ satisfies the same boundary condition at the spherical surface, has zero normal gradient there, and tends to a linear spatial variation ($\sim 2x/3$) at large distances from the sphere. Thus, it applies to a conductor surrounding an adiabatic sphere. Here it is taken to apply to the solid surrounding the cavity. Its isotherms are shown in figures 1 (a) and 4.

3. Low Grashof Number Expansion

By assuming an asymptotic expansion for the velocity of the form $\mathbf{u} \sim \mathbf{u}_0 + Gr\,\mathbf{u}_1 + Gr^2\mathbf{u}_2 + \cdots$ as $Gr \to 0$, with Pr fixed and finite, and similar forms for T and p, (1–3) give a sequence of Poisson and inhomogeneous Stokes equations for the corrections to the temperature and velocity, respectively. Apart from the conduction temperature field, T_0, which satisfies (4), the fields T_i and $\mathbf{u}_i$ satisfy homogeneous Dirichlet boundary conditions.

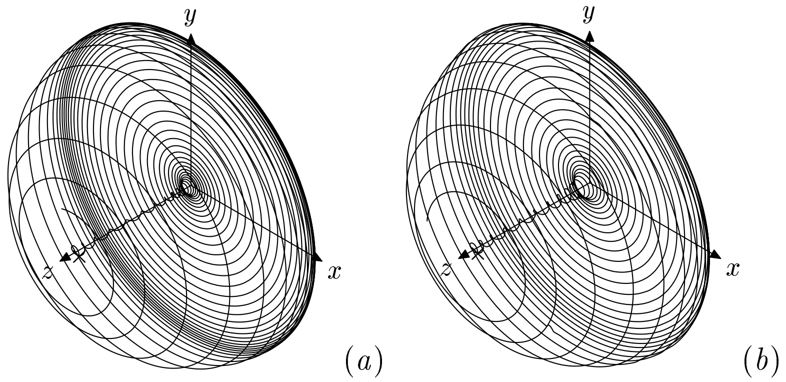

Figure 2: Particle track in steady flow in a horizontally heated sphere at Ra=1000, Pr=0.7, as predicted (a) from the first-order velocity field, $\mathbf{u} \sim \mathbf{u}_0 + Gr\mathbf{u}_1$, and (b) from the numerical solutions.

The results, as derived previously [8, 9], for the conduction temperature, T_0, the creeping flow, $\mathbf{u}_0$, the first-order temperature correction, T_1, and the first-order velocity corrections due to inertia, $\mathbf{u}_{1I}$ and buoyancy, $\mathbf{u}_{1B}$ are:

$$T_0 = x; \tag{5}$$

$$\mathbf{u}_0 = \frac{r(1-4r^2)}{80}\sin\theta\hat{\boldsymbol{\phi}}; \tag{6}$$

$$T_1 = \frac{Pr}{44\,800}r(1-4r^2)(9-20r^2)\sin\theta\sin\phi; \tag{7}$$

$$\mathbf{u}_{1I} = \frac{r(1-4r^2)}{106\,444\,800}\Big[(1-4r^2)(28r^2-19)(3\cos^2\theta-1)\,\hat{\boldsymbol{r}} +3(336r^4-224r^2+19)\sin\theta\cos\theta\,\hat{\boldsymbol{\theta}}\Big] \tag{8}$$

$$\mathbf{u}_{1B} = \frac{Pr\ r(1-4r^2)}{106\,444\,800}\left[(1-4r^2)(23-20r^2)(3\cos^2\eta-1)\hat{\boldsymbol{r}} -3(240r^4-248r^2+23)\sin\eta\cos\eta\hat{\boldsymbol{\eta}}\right] \tag{9}$$

4. Second-order Temperature Correction

The second-order temperature correction satisfies $A_2 = \nabla^2 T_2$ and vanishes on the boundary. The 'source' term A_2 has three parts: $A_2 = A_{2I}+A_{2B}+A_{2U} \equiv Pr(\mathbf{u}_{1I}\cdot\boldsymbol{\nabla}T_0+\mathbf{u}_{1B}\cdot\boldsymbol{\nabla}T_0+\mathbf{u}_0\cdot\boldsymbol{\nabla}T_1)$ where

$$A_{2I} = \frac{Pr\ r(1-4r^2)}{106\,444\,800}\left[112r^4-104r^2+19+(672r^4-360r^2)\cos^2\theta\right]\sin\theta\cos\phi \tag{10}$$

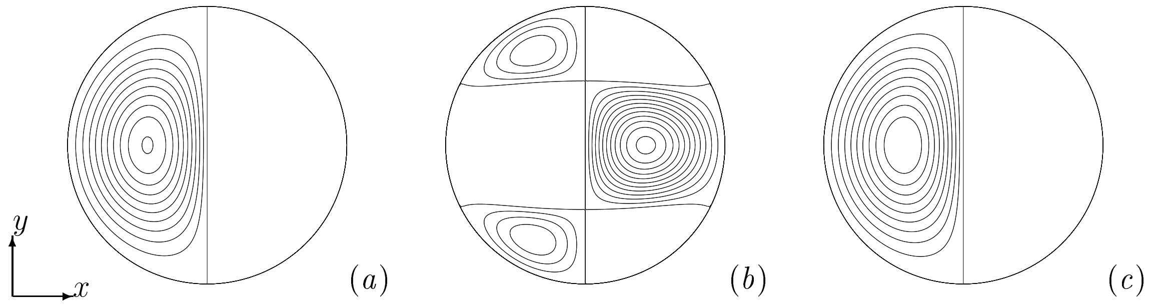

Figure 3: Second-order corrections to the temperature field in the plane $z = 0$ due to (a) inertia, T_{2I}, (b) buoyancy, T_{2B}, and (c) and the base flow, T_{2U}. The negative isotherms are not shown; each field is odd-symmetric about the zy-plane.

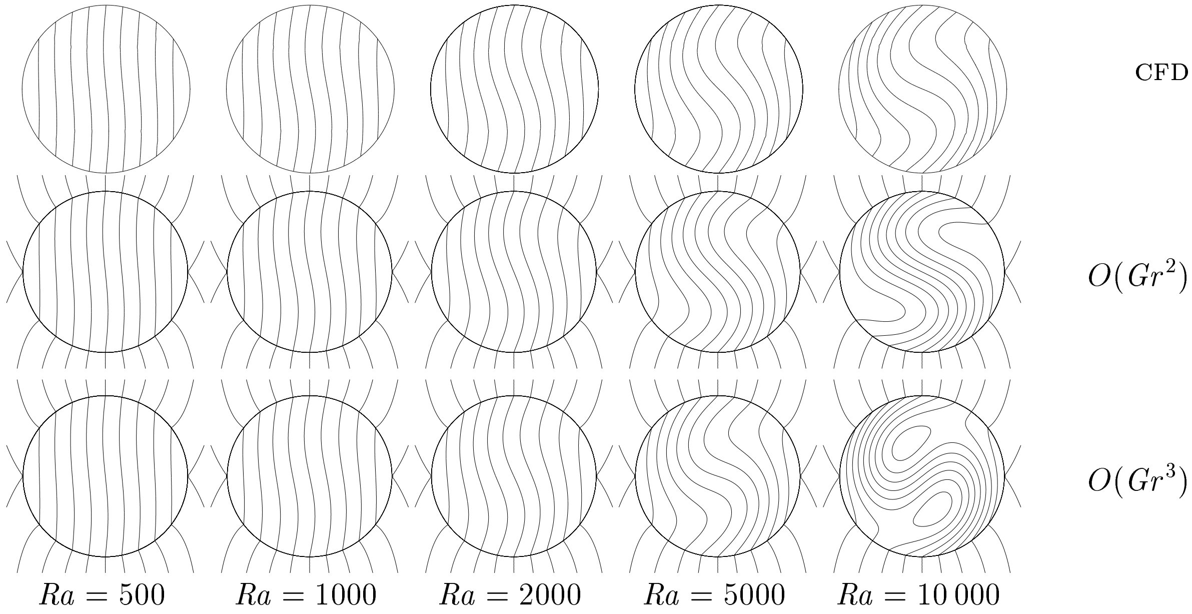

Figure 4: Isotherms in the plane $z = 0$ for $Pr = 0.7$; see figure 1 (a) for key. The top row is the numerical solutions and the second and third are first- $(T \sim T_0 + GrT_1)$ and second-order $(\ldots + Gr^2 T_2)$ asymptotic approximations.

$$A_{2B} = \frac{Pr^2\, r(1-4r^2)}{106\,444\,800}\left[24r^2(20r^2-17)\sin^2\eta - (560r^4 - 520r^2 + 23)\right]\sin\eta\sin\upsilon \quad (11)$$

$$A_{2U} = -\frac{Pr^2}{3\,584\,000}(1-4r^2)^2(9-20r^2)\sin\theta\cos\phi. \quad (12)$$

It is convenient to consider separately the temperature fields corresponding to each of these source fields. These are hereafter denoted T_{2I}, T_{2B} and T_{2U}. The solutions, which were obtained by means of spherical harmonics [12], are:

$$T_{2I} = \frac{Pr\, r(1-4r^2)}{221\,405\,184\,000}\,[20\,160r^6 - 24\,080r^4 + 6980r^2 - 299 \\ -160r^2(4r^2-3)(28r^2-11)\sin^2\theta]\sin\theta\cos\phi \quad (13)$$

$$T_{2B} = \frac{Pr^2\, r(1-4r^2)}{664\,215\,552\,000}\,[160r^2(240r^4 - 408r^2 + 119)\sin^2\eta \\ -43\,2000r^6 + 76\,560r^4 - 25\,060r^2 + 1131]\sin\eta\sin\upsilon \quad (14)$$

$$T_{2U} = \frac{Pr^2\, r(1-4r^2)\,(302\,400r^6 - 392\,560r^4 + 175\,100r^2 - 31\,069)}{1\,192\,181\,760\,000}\sin\theta\cos\phi. \quad (15)$$

The isotherms in the plane $z = 0$ are displayed in figure 3.

The combined first- and second-order asymptotic approximations of the temperature field in the plane $z = 0$ are illustrated in figure 4 for various Rayleigh numbers, $Ra \equiv Gr\,Pr$. The approximations at the higher values of Ra are increasingly suspect; closed isotherms (as evinced by the second-order approximation at $Ra = 10\,000$) are not possible for the true solution [8, 13]. For some appreciation of the Rayleigh numbers likely to be encountered: for air at 300 K, $\Delta T = 10$ K across a 1 cm cavity gives $Ra \approx 920$, for water, however, Ra would be 2×10^5.

5. Overall Heat Transfer Rate

The temperature field T_0 yields the conduction heat transfer rate, which is taken as the basis

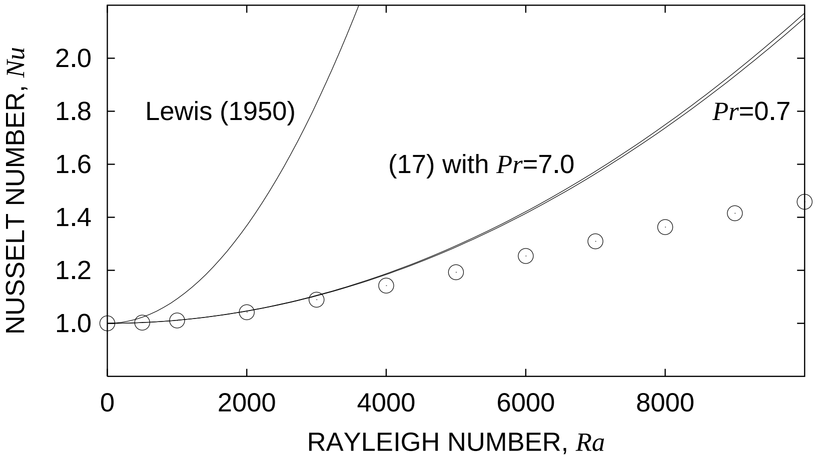

Figure 5: Overall heat transfer rate across the sphere. The curves show asymptotic predictions while the discrete points $\odot$ are the results of numerical simulations at $Pr = 0.7$.

for normalization. The Nusselt number is therefore defined as:

$$Nu \equiv \frac{1}{\pi} \int_{-\pi/2}^{\pi/2} \int_0^{\pi} (\hat{\boldsymbol{r}} \cdot \boldsymbol{\nabla} T)\big|_{r=\frac{1}{2}} \sin\theta \mathrm{d}\theta\, \mathrm{d}\phi; \tag{16}$$

i.e. the integral of the conduction flux over the hemisphere $x \geq 0$.

The first-order thermal correction T_1 does not contribute to the Nusselt number. Indeed, the Nusselt number must be an even function of the Grashof number [8]. Thus, the second-order correction to the temperature field obtained in the present paper delivers the lowest-order correction to the Nusselt number. It yields

$$Nu \sim 1 + Gr^2 Pr^2 \left(\frac{4259}{363\,242\,880\,000} - \frac{1}{6\,918\,912\,000 Pr} \right) + O(Gr^4). \tag{17}$$

Almost 99% of the correction to Nu is due to the interaction of the primary flow, $\mathbf{u}_0$, and the basic disturbance to the conduction temperature field. The relatively unimportant term inversely proportional to Pr is a purely three-dimensional effect, resulting from the secondary inertially generated axial flow.

This prediction may be compared with that obtained by Lewis [10], $Nu \sim 1 + 9.21875 \times 10^{-5} Ra^2$, which is also drawn in figure 5. The error associated with treating three-dimensional natural convection as planar is clear.

6. Numerical Solutions

The flow was also simulated using a commercial CFD code [14]. The code solves general flow problems using the finite volume method. The governing equations (1–3), subject to $\mathbf{u} = \mathbf{0}$ and (4) at $r = \frac{1}{2}$, were discretized over the mesh shown in figure 1 (b), and solved by the SIMPLEC scheme [15]. Taking advantage of the symmetry of the solutions, only the hemisphere $z > 0$ was modelled.

A quasiuniform mesh of 5888 volumes was used. To reduce the residual (apparent mass source) of the discretized continuity equation (1) to less than the stipulated tolerance of 10^{-5} took approximately 5000 iterations and 40 minutes of CPU time on a single Compaq EV6 466 MHz processor.

Each solution was started with an initial guess of a uniform zero temperature field. For higher Grashof numbers ($Gr > 2000$), an underrelaxation factor of 0.8 had to be applied to the temperature to obtain a converged solution.

With any simulation, it is important to assess the effect of grid refinement [16]. A mesh independence check was performed using a mesh of 47 104 quasiuniformly distributed volumes. The maximum observed nodal speed for each Grashof numbers changed by less than 1.6%, so that the solution on the original mesh is considered essentially mesh-independent. The overall heat transfer rate changed by less than 0.4%.

7. Conclusion

The asymptotic approximation for the temperature field in natural convection in a spherical cavity in a horizontally heated perfectly conducting solid has been extended to second-order in the Grashof number. This contributed the first nonzero correction to the overall heat transfer rate. Comparison with numerical results indicated that the second-order approximation to the Nusselt number predicts the convective increase in the heat transfer rate to within 5% for $Ra < 4000$, after which the true Nusselt number increases more slowly than Ra^2.

8. References

[1] Bejan, A., 1995: Convection Heat Transfer. Wiley, 2nd edition, ch. 5.

[2] Gill, A. E., 1966: The boundary-layer regime for convection in a rectangular cavity. *J. Fluid Mech.*, 26, 515–536.

[3] Mallinson, G. D., and G. de Vahl Davis, 1973: The method of the false transient for the solution of coupled elliptic equations. *J. comput. Phys.*, 12, 435–461.

[4] Mallinson, G. D., and G. de Vahl Davis, 1977: Three-dimensional natural convection in a box: A numerical study. *J. Fluid Mech.*, 83, 1–31.

[5] de Vahl Davis, G., 1998: Unnatural natural convection. In Leonardi, E. and Madhusudana, C. V., eds, Heat and Mass Transfer Australasia 1996, pp. 1–16. Begell House, New York.

[6] Morrison, G. L., and V. Q. Tran, 1978: Laminar flow structure in vertical free convective cavities. *Int. J. Heat Mass Transfer*, 21, 203–213.

[7] Hiller, W. J., S. Koch and T. A. Kowalewski, 1989: Three-dimensional flow structures in laminar natural convection in a cubic enclosure. *Expl thermal Fluid Sci.*, 2, 34–44.

[8] McBain, G. D., 1999: Vapour transport across gas-filled enclosures. PhD thesis, James Cook University, Townsville.

[9] McBain, G. D., (submitted for publication): Convection in a horizontally heated sphere. J. Fluid Mech.

[10] Lewis, J. A., 1950: Free convection in commerical insulating materials. PhD thesis, Brown University, Providence.

[11] Ostroumov, G. A., 1958: Free convection under the conditions of the internal problem. Technical Report TM 1407, NACA. Trans. S. Reiss.

[12] Lamb, H., 1932: Hydrodynamics. Cambridge University Press, 6th edn, ch. 5.

[13] McBain, G. D., (in press): Spatial extrema of advected scalars. *Int. J. Heat Mass Transfer.*

[14] CFX International, 1997: CFX-4.2 Solver Manual. Harwell, Didcot, Oxfordshire.

[15] van Doormal, J. P., and G. D. Raithby, 1984: Enhancements of the SIMPLE method for predicting incompressible fluid flows. *Num. Heat Transfer*, 7, 147–163.

[16] Freitas, C. J., 1993: Editorial. *J. Fluids Engng*, 115, 339.